Optical Engineering

OpticalEngineering.SPIEDigitalLibrary.org

Optical metrology of a large deformable aspherical mirror using software configurable optical test system

Run Huang
Peng Su
Todd Horne
Guido Brusa
Jim H. Burge

SPIE.

Optical metrology of a large deformable aspherical mirror using software configurable optical test system

Run Huang,[a,*] Peng Su,[a] Todd Horne,[a] Guido Brusa,[b] and Jim H. Burge[a]
[a]The University of Arizona, College of Optical Sciences, Tucson, Arizona 85721, United States
[b]The University of Arizona, Steward Observatory and Large Binocular Telescope, Tucson, Arizona 85721, United States

Abstract. The software configurable optical test system (SCOTS) is an efficient metrology technology based on reflection deflectometry that uses only a liquid-crystal display and a camera to measure surface slope. The surface slope is determined by triangulation using the co-ordinates of the display screen, camera, and test mirror. We present our SCOTS test results concentrated on high dynamic range measurements of low order aberrations. The varying astigmatism in the 910-mm diameter aspheric deformable secondary mirror for the large binocular telescope was measured with SCOTS, requiring no null corrector. The SCOTS system was designed on-axis with camera and screen aligned on the optical axis of the test mirror with the help of a 6-inch pellicle beam splitter. The on-axis design provides better control of the astigmatism in the test. The high dynamic range of the slope provided a measurement of astigmatism within 0.2-μm root-mean-square accuracy in the presence of 231-μm peak-to-valley aspheric departure. The simplicity of the test allowed the measurements to be performed at multiple gravity angles. [DOI: 10.1117/1.OE.53.8.085106]

Keywords: deflectometry; optical metrology; aspheric; software configurable optical test system.

Paper 140673P received Apr. 23, 2014; revised manuscript received Jul. 13, 2014; accepted for publication Jul. 16, 2014; published online Aug. 15, 2014.

1 Introduction

Interferometry has served as an accurate noncontact optical metrology technology for a long time. The wave nature of light gives this technology subwavelength precision and accuracy; however, it typically has a small dynamic range. Traditional null testing interferometry can only measure the surface departures within a few wavelengths from reference shapes. For measuring aspheric or freeform optics, interferometry usually requires compensation optics such as a computer-generated hologram. Sometimes a stitching process is also required for measuring large aspheric optics, which makes interferometry testing costly and inflexible. In addition, interferometry requires a normal incidence that leads to tedious alignment and calibration to perform accurate testing.[1,2] The software configurable optical test system (SCOTS), a slope measurement technique based on deflectometry, provides a contact-free, high dynamic range, full field metrology method with easy system setup and alignment. It is able to achieve high dynamic range slope measurements by using computer-controlled large displays such as liquid-crystal display (LCD) monitors. The camera in SCOTS provides a full-field of view of the test optics and a 2-D surface map can be obtained within one measurement, thus, no stitching is needed. The performance of SCOTS has been successfully demonstrated in testing many large astronomy telescope mirrors and precision x-ray mirrors.[3–7]

In this paper, we show SCOTS test results for a 910-mm diameter aspheric deformable secondary mirror for the large binocular telescope (LBT).[8,9] The observatory noticed an elevation dependent astigmatism in its secondary. A compact SCOTS system was taken to the observatory to further investigate this aberration. A series of tests demonstrated that the SCOTS accurately measured the astigmatism to submicrometer accuracy in the presence of a 231-μm peak-to-valley aspheric departure.

The paper is organized as follows. In Sec. 2, we describe the principle of SCOTS as a Hartmann test in reverse. In Sec. 3, we provide a detailed discussion of the system design, expected performance, alignment procedures, and test results. Conclusions are given in Sec. 4.

2 Principle

SCOTS uses deflectometry to measure slopes by triangulation. It works like a Hartmann test[10] but in reverse. Figure 1 shows the schematic comparison of Hartmann and SCOTS tests. In a Hartmann test, a point source of light is placed near the center of curvature of the test mirror, and a plate with a number of holes is centered just in front of the test mirror. The point source illuminates the entire test mirror, but only the light passing through the holes is reflected. One or more images are recorded for slope calculations. In SCOTS, the detector in Hartmann test is replaced by an LCD screen and the point source is replaced by a camera focusing on the test mirror to detect the light reflected from the display.

When testing a polished optical surface, we are usually interested in the surface departure of the testing surface from its ideal shape. We approximate the wavefront slopes to be equal to Eq. (1) based on the transverse ray aberration model[11]

$$\frac{\partial W(x,y)}{\partial x} \cong -\frac{\Delta x_{\text{screen}}}{d_{m2\,\text{screen}}}, \frac{\partial W(x,y)}{\partial y} \cong -\frac{\Delta y_{\text{screen}}}{d_{m2\,\text{screen}}}, \quad (1)$$

*Address all correspondence to: Run Huang, E-mail: rhuang@optics.arizona.edu

0091-3286/2014/$25.00 © 2014 SPIE

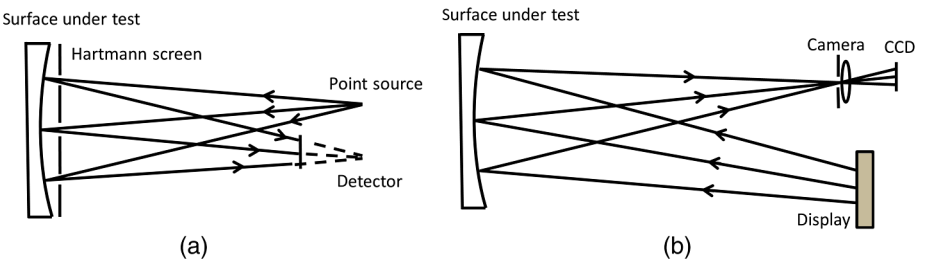

Fig. 1 Schematic setup of (a) a Hartmann test and (b) a software configurable optical test system (SCOTS) test. SCOTS traces rays in reverse.

$$\Delta x_{\text{screen}} = x_{\text{measured}} - x_{\text{ideal}} \quad \Delta y_{\text{screen}} = y_{\text{measured}} - y_{\text{ideal}}, \tag{2}$$

where $W(x, y)$ is the wavefront aberration and $d_{m2\,\text{screen}}$ is the distance from the mirror to the display. The measured x and y positions (x_{measured} and y_{measured}) are determined by phase shifting or line scanning techniques.[3] The ideal x and y positions (x_{ideal} and y_{ideal}) are determined by ray tracing for the case of an ideal optical surface. From these slopes, a wavefront map is reconstructed by zonal integration.

3 SCOTS Test for a Large Deformable Aspherical Mirror

3.1 *On-Axis SCOTS*

As mentioned in Sec. 1, the LBT secondary mirror is an $f/1.1$ deformable ellipsoid with a 910-mm diameter and a 231-μm aspheric departure. Although SCOTS allows an off-axis configuration as shown in Fig. 1(b), sensitivity to alignment errors can be reduced by maintaining coaxial alignment of the camera, display, and test mirror for measuring axisymmetric mirrors. The dominant aberration in the LBT secondary is astigmatism and it can be described using Seidel sums as[12]

$$W_{222} = \frac{1}{2} S_{\text{III}}, \tag{3}$$

$$S_{\text{III}} = -\sum \bar{A}^2 y \Delta\left(\frac{u}{n}\right), \tag{4}$$

$$\bar{A} = n\bar{u} + n\bar{y}c, \tag{5}$$

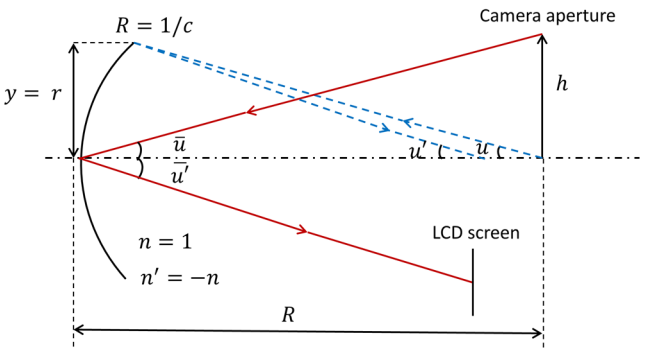

Fig. 2 Ray tracing in SCOTS for Seidel coefficient calculation.

$$\Delta\left(\frac{u}{n}\right) = \left(\frac{u'}{n'}\right) - \left(\frac{u}{n}\right), \tag{6}$$

where $\bar{y}$ is chief ray height, y is marginal ray height, $\bar{u}$ and $\bar{u}'$ are the chief ray angles before and after reflection, and u and u' are marginal ray angles before and after reflection, respectively.

Applying Eqs. (3)–(6) to a SCOTS test, two rays are traced through the system, the marginal ray for full aperture (Fig. 2 dashed ray, $y = r$) and the chief ray (Fig. 2 solid ray, $\bar{y} = 0$) at the maximum field, (i.e., the camera off-axis distance, h). Using the paraxial approximation, we can get an astigmatism of

$$W_{222} = \frac{h^2 r^2}{R^3}. \tag{7}$$

The sensitivity of astigmatism to the camera off-axis distance is

$$\frac{\partial W_{222}}{\partial h} = \frac{2\ hr^2}{R^3}. \tag{8}$$

Equation (8) shows that the alignment sensitivity of astigmatism to test geometry increases linearly as a function of the off-axis distance of the camera. Figure 3 plots the sensitivity for LBT secondary mirror SCOTS test. If we use a test geometry with the camera at a 100-mm off-axis distance (i.e., $h = 100$ mm) and have a 0.1-mm uncertainty of camera lateral position, there will be a 0.5-μm uncertainty for W_{222} in the measurement. However, if we use an on-axis geometry (i.e., $h = 0$ mm), a 0.1-mm camera lateral distance

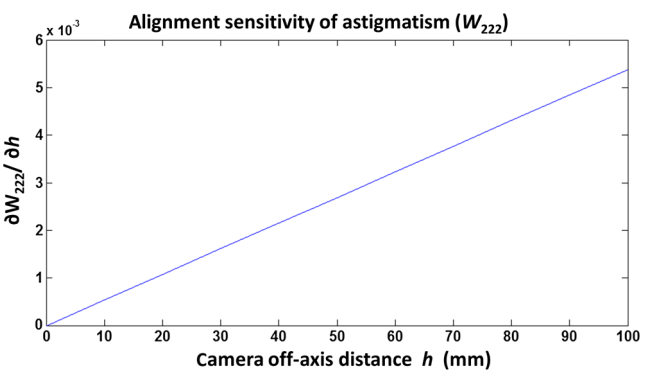

Fig. 3 A plot showing the SCOTS alignment sensitivity of astigmatism due to the camera off-axis distance for the large binocular telescope secondary mirror.

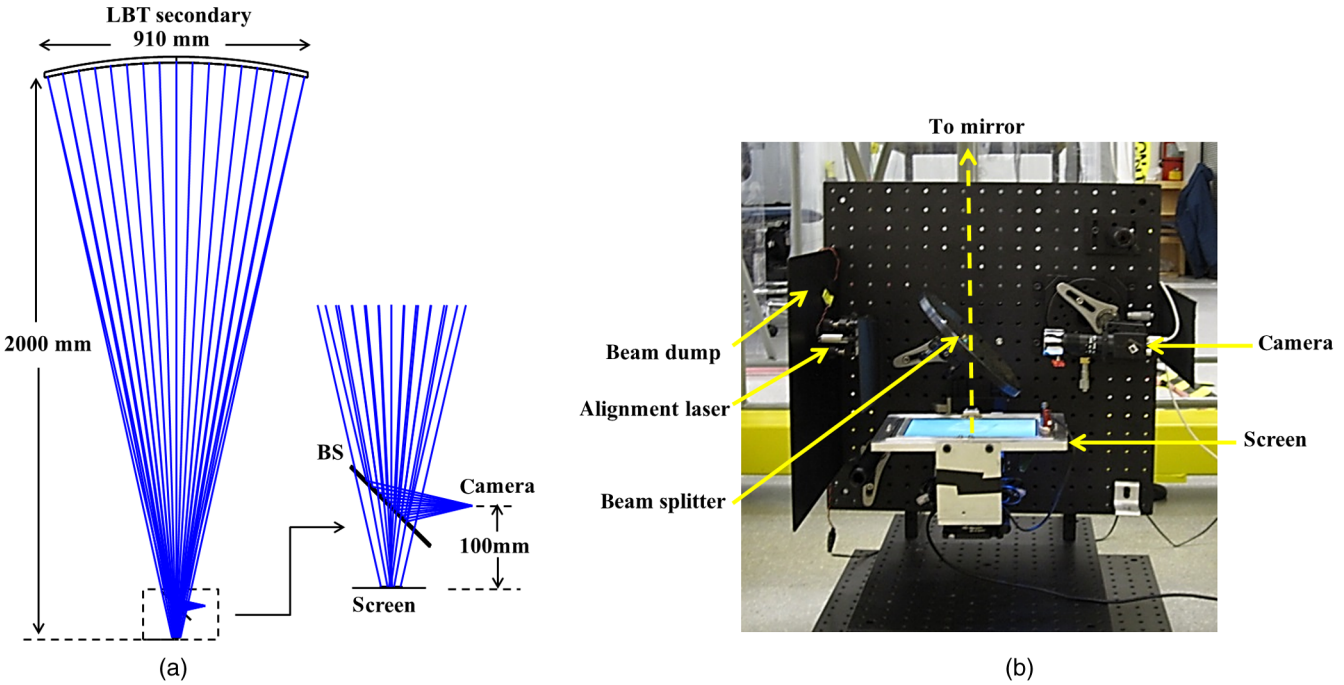

Fig. 4 (a) Geometry layout of the on-axis SCOTS test and (b) experiment setup.

uncertainty will only generate a 0.3-nm uncertainty for W_{222} in the test. Therefore, an on-axis design makes the SCOTS test less sensitive to geometric uncertainty in component positions and reduces test geometry induced astigmatism in the measurements.

It is worth mentioning that the coaxial alignments of the camera, LCD, and the test mirror also makes the camera view of the test mirror free from perspective distortion which is a major difficulty with many SCOTS tests and has to be calibrated out by putting customized fiducial targets on the test mirror.[5]

The on-axis SCOTS setup for the LBT secondary mirror measurement is shown in Fig. 4. A 7-inch mini LCD screen with a 190.5-μm pixel pitch is aligned at the center of curvature of the secondary mirror to illuminate the test mirror; a 6-inch pellicle beam splitter with a 2-μm thickness is set between the screen and test mirror and is 100 mm away from the LCD screen. A camera is put into the reflection path of the beam splitter. The camera lens has a 1-mm external aperture and a 6-mm focal length with a 42-deg field-of-view. The distance between the camera and the beam splitter is also set at 100 mm. An alignment laser is placed opposite to the camera and is used for creating a reference axis in the alignment, which will be discussed in detail in Sec 3.3. A beam dump is also used to prevent stray light from entering the camera.

3.2 *Effect of Beam Splitter*

As stated in Sec 3.1, the use of a pellicle beam splitter makes the test components coaxial to reduce the sensitivity of the test to alignment. However, the beam splitter inherently adds errors to the measurement due to its thickness and shape variation. In this section, we will discuss the effects of these two potential issues in the LBT secondary SCOTS test.

To consider the effect of constant thickness, the beam splitter is treated as a plane parallel plate (PPP), which causes a lateral displacement of the rays passing through it. For small angles, the lateral displacement D can be approximated as[13]

$$D \approx \frac{TI(n-1)}{n}, \tag{9}$$

where T is the thickness of the beam splitter and I is the incident angle on the beam splitter.

When a PPP is used with collimated light, no aberration is introduced. However, as shown in Fig. 5, and in a SCOTS test, the beam splitter is used with converging light where astigmatism, coma, and spherical aberrations arise. To compute the magnitude of this effect in the test, we added 2 μm

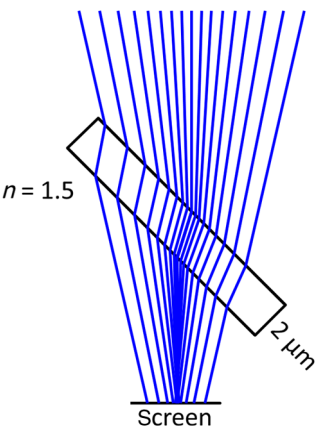

Fig. 5 The constant thickness of the beam splitter introduces aberrations when it is used with converging light.

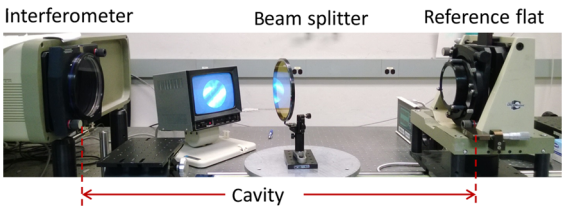

Fig. 6 Experiment setup to measure the thickness variation of the pellicle beam splitter.

to the thickness of the beam splitter in the LBT secondary SCOTS test model using ZEMAX. The ray trace result showed that it merely generated 3.4-nm RMS wavefront errors (mainly astigmatism). Therefore, the measurement error coming from the constant thickness of the beam splitter can be ignored for this test because it did not require nanometer level accuracy.

The thickness variation of the beam splitter was measured in transmission with a Fizeau interferometer as shown in Fig 6. The difference map [Fig. 7(a)] shows that there are low order thickness fluctuations (2 to 4 cycles/aperture) in the beam splitter. Figure 7(b) is the integrated one-dimensional power spectral density plot [PSD(υ)] of the difference map [Fig. 7(a)]. Using Eq. (10), the RMS value at a certain spatial frequency can be calculated[14]

$$\mathrm{rms} = \sqrt{\int_{\upsilon 1}^{\upsilon 2} \mathrm{PSD}(\upsilon) d\upsilon}. \tag{10}$$

Based on the above experiment and PSD analysis, three sine shape surface sags at 1, 4, and 10 cycles/aperture with RMS amplitude of 3, 0.5, and 0.05 nm, respectively, were added to the front surface of the beam splitter in the LBT secondary SCOTS ZEMAX model. The ray trace result showed that the introduced measurement error was on the level of 1-nm RMS for the wavefront and 10^{-8} rad for the wavefront slope, which was also negligible.

The experiments and analysis above are general and may be extended to similar deflectometry systems using a beam splitter to make an on-axis alignment. It will help to quantify and budget the effect of a beam splitter during test design.

Table 1 Tolerance analysis for large binocular telescope secondary mirror on-axis SCOTS test.

Wavefront (unit: μm)	Camera lateral shift 1 mm	Mirror tilt 0.35 deg	Mirror z shift 20 mm	Screen tilt 0.3 deg	Root sum square
Z5 (astigmatism)	0	0	0	0	0
Z6 (astigmatism)	0.005	0.78	0	0.001	0.78
Z7 (coma)	0.011	0.19	0	0.056	0.20
Z8 (coma)	0	0	0	0	0
Z9 (trefoil)	0	0	0	0	0
Z10 (trefoil)	0	0	0	0	0
Z11 (spherical)	0	0.006	0.21	0	0.21

3.3 *System Alignment*

The observatory required better than 1-μm RMS sensitivity in the measurement of astigmatism. Therefore, we designed the mechanics and the alignment procedure based on the tolerance analysis in Table 1. The tolerance shows that the astigmatism is very sensitive to the mirror tilt, whereas it is insensitive to the screen tilt and the longitudinal distance from SCOTS to the mirror.

The designed alignment was separated into two steps. The first step was the in-lab integration of the SCOTS package with prealignment of the components. The second step was the alignment of the test mirror and the SCOTS package at the observatory.

An alignment laser, placed on the opposite side of the beam splitter to the camera (depicted in Fig. 8), shot a collimated beam to the beam splitter with 50% of the light transmitted and 50% reflected. The laser beam served as the reference optical axis for the whole system. The first step of the prealignment (Fig. 8①) was to align the camera's

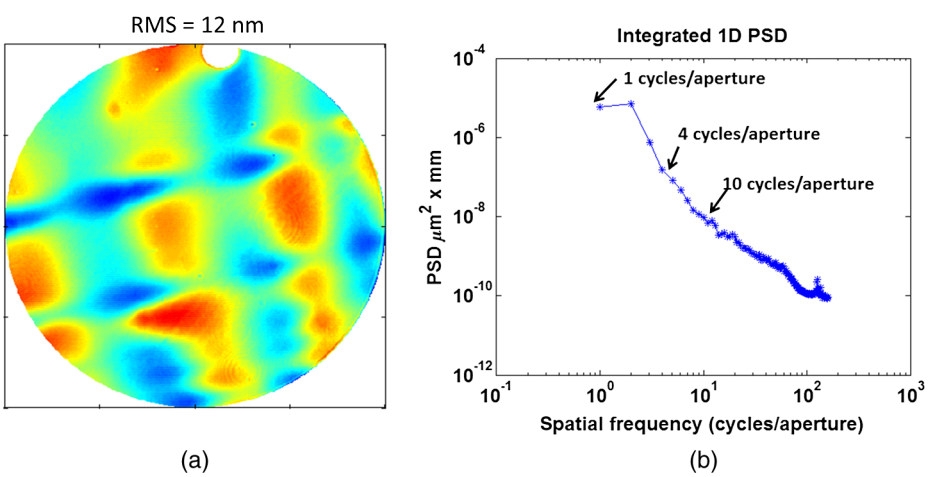

Fig. 7 (a) Difference map with and without beam splitter in the light path. (b) One-dimensional power spectral density of (a).

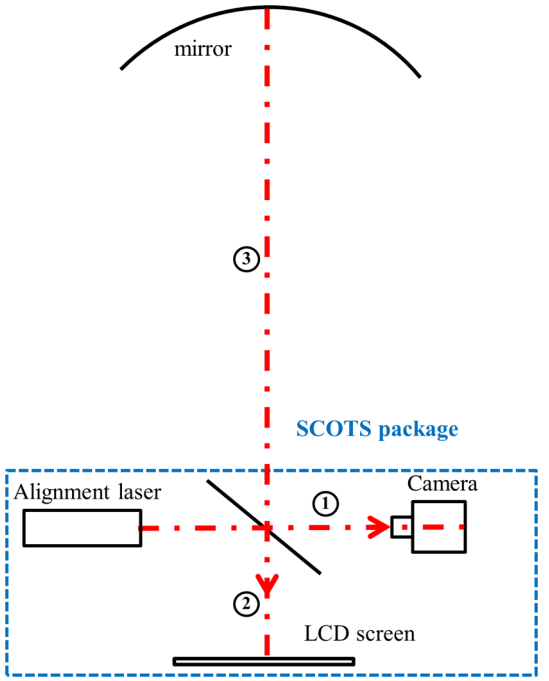

Fig. 8 Alignment of SCOTS test. The SCOTS package was prealigned before taken to the observatory. The on-axis alignment was achieved with the help of an alignment laser.

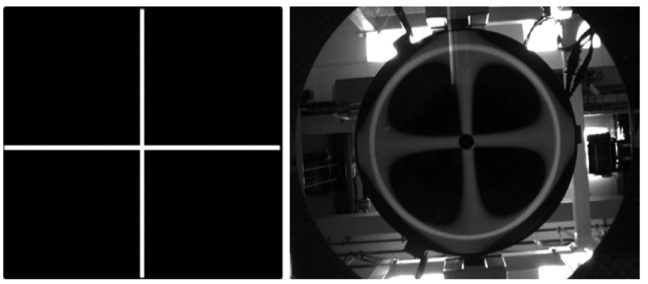

(a) (b)

Fig. 9 (a) A bright cross on the screen was lit up to illuminate the mirror. (b) Reflected image of the cross on the mirror.

aperture and the center of the CCD onto the laser beam. The camera was translated so that the laser beam with ~1-mm diameter was able to go through the 1-mm external aperture of the camera. Subsequently, by tip-tilting the camera and monitoring the centroid of the laser beam incident on the CCD, the laser beam was positioned at the center of the camera sensor within a 0.1-pixel accuracy. The second step of the prealignment (Fig. 8②) was to align the LCD screen perpendicular to the laser beam by adjusting its tip-tilt so that the laser beam reflected by the screen went back through the aperture of the alignment laser. The position where the laser beam was incident on the LCD screen was recorded for the second alignment step. With these prealignment steps, the SCOTS package was sent to the observatory.

Once at the LBT observatory, the SCOTS package had to be aligned with the secondary mirror (Fig. 8③) so that (1) the mirror was centered on the CCD and (2) the mirror was perpendicular to the SCOTS axis. The mirror centering was controlled to ~0.2-mm accuracy by fitting a circle to the image of the mirror boundary where the center of the circle could be calculated with sub pixel accuracy. The major challenge in aligning the secondary mirror normal to the reference optical axis was the central obscuration on the mirror, which made it impossible to use a vertex reflection of the laser beam. Instead, we used a bright cross [see Fig. 9(a)] produced by the LCD screen at the previously recorded position. By adjusting the mirror tip-tilt and having both the mirror and the reflected cross centered on the CCD, [as shown in Fig. 9(b)], the mirror was aligned with its vertex perpendicular to the optical axis. Considering the limitation of the mechanical mounting of the mirror and the width of the reflected cross, we estimated the mirror tilt was aligned within 0.1-deg accuracy.

With the two-step alignment procedures, the test setup was aligned within the tolerance and was capable of measuring astigmatism with submicrometer accuracy.

3.4 *Test Results*

The performance of the low-order aberration measurement of this SCOTS was first verified with the secondary mirror pointing straight down as shown in Fig. 10(a). Intensity

(a) (b)

Fig. 10 SCOTS test of the secondary mirror with mirror (a) pointing straight down and (b) at 30-deg elevation position.

sinusoidal fringes were displayed on the LCD screen in the x and y directions and a four-step phase-shifting algorithm was used to register the mirror pixel coordinates with the screen pixel coordinates. Figure 11 shows camera captured raw intensity maps of the sinusoidal fringes reflected by the mirror and Fig. 12 shows the calculated LCD screen position. At this position, SCOTS measured ~0.2-μm (RMS) astigmatism. This 0.2 μm (RMS) might be the combined effect from the alignment uncertainty, the systematic error in SCOTS, and a small amount of inherent errors in the secondary mirror.

After the initial measurement, a series of controlled aberration, 1-μm astigmatism (RMS), 1-μm coma (RMS), and 1-μm trefoil (RMS) wavefront errors were intentionally added using the deformable secondary mirror and SCOTS accurately measured these aberrations with submicrometer accuracy. The wavefront maps shown in Fig. 13 are the commanded wavefronts, measured wavefronts, and the difference. The repeatability of the test is 2-μrad RMS in slope and 98-nm RMS in wavefront, taking measurements at the same test configuration several times.

After the verification tests with the secondary mirror pointing straight down, this compact SCOTS system was then used to measure the secondary mirror at a different elevation. Figure 10(b) shows the test configuration at a 30-deg elevation (i.e., optical axis at 60-deg from vertical). Moving the mirror to a 30-deg elevation introduced a large amount of astigmatism, the value of which is a function of the path followed (hysteresis). As shown in Table 2, reaching a 30-deg elevation from the vertical position caused an ~6.2-μm RMS astigmatism but only an ~3.7-μm RMS astigmatism when the position was reached from horizon pointing (i.e., optical axis horizontal). This test result confirmed previous measurements taken with the unit installed at the telescope, including the hysteretic behavior of the introduced aberration. Several other SCOTS measurements were also done after modifying the secondary mirror hardware configuration in an attempt to determine the causes of this aberration. Although no direct cause was found, the measurements eliminated several potential causes. The results obtained will help the observatory design a series of tests to further investigate the source of the astigmatism.

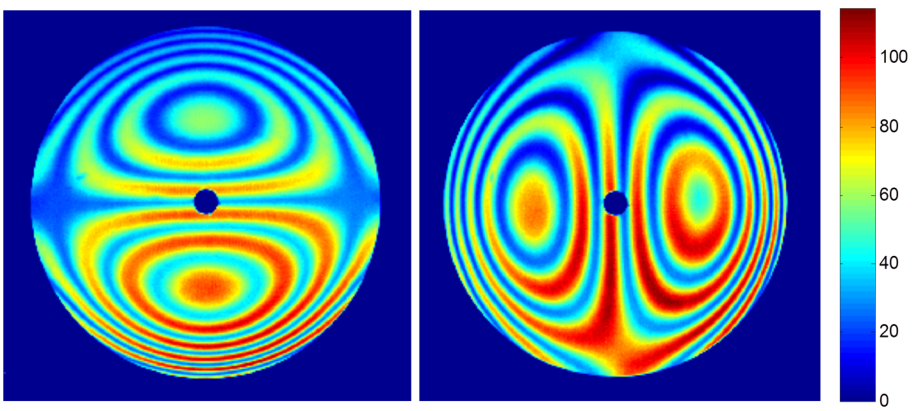

Fig. 11 Raw intensity images of the sinusoidal fringes reflected by the mirror.

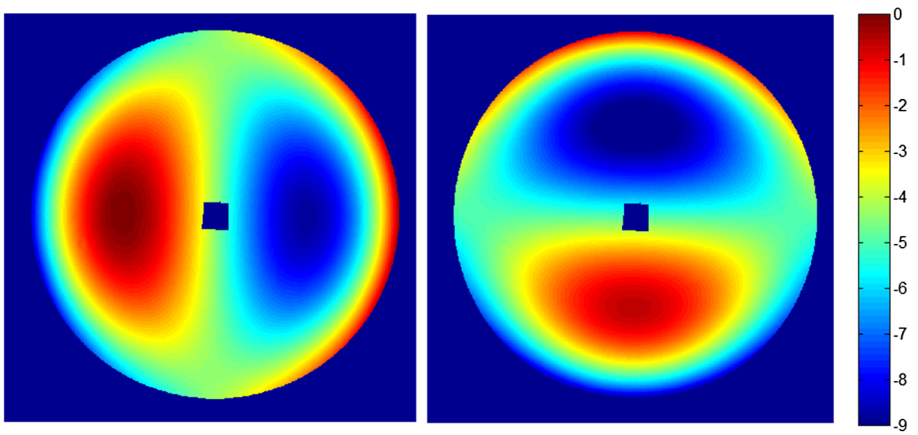

Fig. 12 Measured liquid-crystal display screen position in x and y directions (unit: mm). Those positions were calculated by phase unwrapping algorithm. The secondary mirror is an $f/1.1$ ellipsoid with 231-μm aspheric departure, so the measured wavefront was dominated by spherical aberration and consequently the above patterns show a coma shape (SCOTS directly measures the slopes of wavefront).

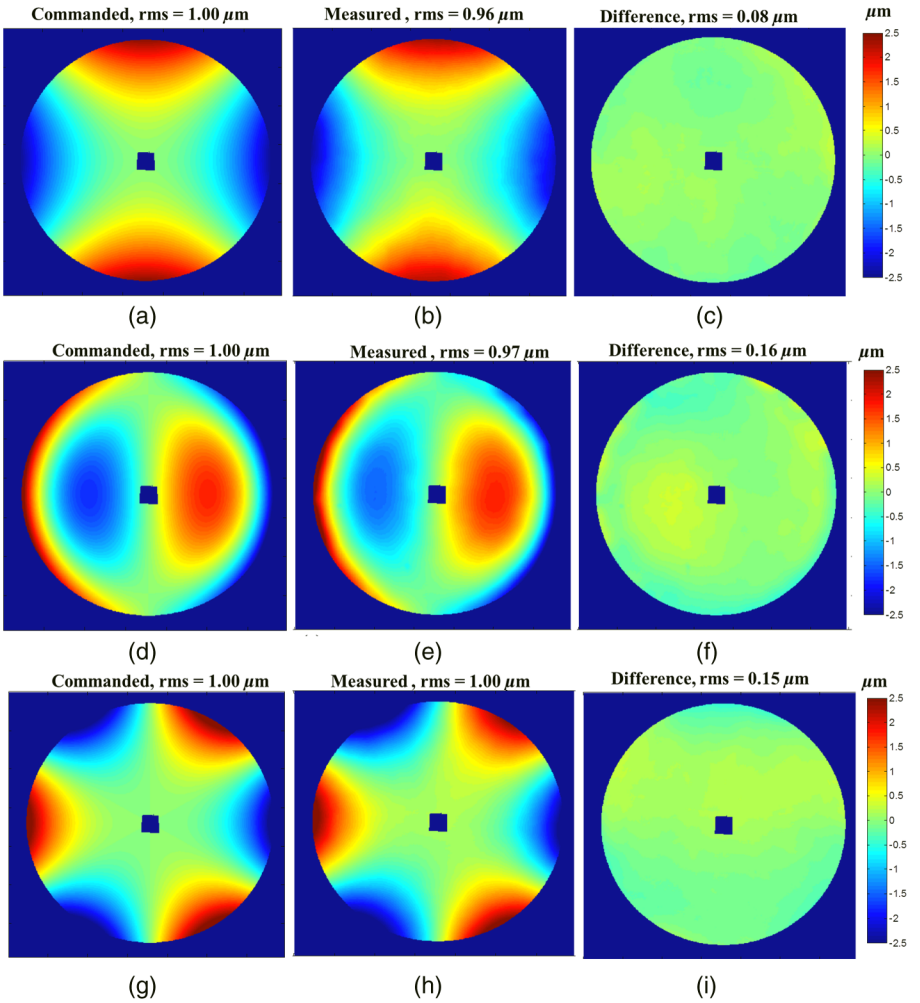

Fig. 13 SCOTS measurement results with controlled aberration in secondary mirror. Unit: μm. (a), (d), and (g) are commanded wavefront aberrations which are 1-μm RMS astigmatism, 1-μm RMS coma, and 1-μm RMS trefoil, respectively. (b), (e), and (h) are SCOTS measured wavefront aberrations. (c), (f), and (i) are the differences between commanded and measured wavefront aberrations.

Table 2 Measured astigmatism by reaching 30-deg from zenith position and horizon position.

Test sequence	Straight down to 30 deg	Horizon to 30 deg
Astigmatism	6.21 μm	3.75 μm

4 Conclusion

An on-axis SCOTS was successfully constructed to measure low order aberrations in the presence of a large spherical departure with submicrometer accuracy. The SCOTS does not require using a null lens and is very compact, allowing us to easily measure the aberrations at multiple mirror orientations with respect to gravity. Unlike previous SCOTS systems, this new on-axis setup does not require perspective corrections. Furthermore, the use of off-the-shelf products for the LCD screen and camera makes this system cost-effective. A detailed study of the beam splitter was presented, which can help us to budget its effect in future SCOTS tests.

To advance this technology to a higher accuracy level, careful calibrations related to system geometry, lens imaging aberration, stray light, etc., need to be performed. Continuing research on the SCOTS system calibration is being conducted in our group to improve the accuracy of the test to a nm or even a subnanometer RMS.

References

1. M. Knauer, J. Kaminski, and G. Hausler, "Phase measuring deflectometry: a new approach to measure specular free form surfaces," *Proc. SPIE* **5457**, 366–376 (2004).
2. C. Faber et al., "Deflectometry challenges interferometry: the competition gets tougher!," *Proc. SPIE* **8493**, 84930R (2012).
3. P. Su et al., "Software configurable optical test system: a computerized reverse Hartmann test," *Appl. Opt.* **49**(23), 4404–4412 (2010).
4. P. Su et al., "Precision aspheric optics testing with the SCOTS: a deflectometry approach," *Proc. SPIE* **8788**, 87881E (2013).
5. P. Su et al., "SCOTS: A reverse Hartmann test with high dynamic range for giant Magellan telescope primary mirror segments," *Proc. SPIE* **8450**, 84500W-1 (2012).
6. P. Su et al., "Non-null full field x-ray mirror metrology using SCOTS: a reflection deflectometry approach," *Opt. Express* **20**(11), 12393–12407 (2012).
7. R. Huang et al., "X-ray mirror metrology using SCOTS/deflectometry," *Proc. SPIE* **8848**, 88480G (2013).
8. A. Riccardi et al., "The adaptive secondary mirror for the Large Binocular Telescope: optical acceptance test and preliminary on-sky commissioning results," *Proc. SPIE* **7736**, 77362C (2010).
9. R. Huang et al., "Measurement of a large deformable aspherical mirror using SCOTS (Software Configurable Optical Test System)," *Proc. SPIE* **8838**, 883807 (2013).

10. D. Malacara-Doblado and I. Ghozeil, "Hartmann, Hartmann-Shack, and other screen tests," in *Optical Shop Testing*, 3rd ed., D. Malacara, Ed., Wiley Series in Pure and Applied Optics, pp. 361–397, Wiley, New Jersey (2007).
11. J. L. Rayces, "Exact relation between wave aberration and ray aberration," *Opt. Act.* **11**, 85–88 (1964).
12. J. Sasián, *Introduction to Aberrations in Optical Imaging Systems*, Cambridge University Press, New York (2013).
13. J. C. Wyant and K. Creath, "Basic wavefront aberration theory for optical metrology," *Appl. Opt. Opt. Eng.* **11**, S29 (1992).
14. R. N. Youngworth, B. B. Gallagher, and B. L. Stamper, "An overview of power spectral density (PSD) calculations," *Proc. SPIE* **5869**, 58690U (2005).

Run Huang obtained her BS (2007) and MS (2009) in optics from Nanjing University of Science and Technology, China. She is currently a PhD candidate at the College of Optical Sciences at the University of Arizona. She is working on high-precision deflectometry system development.

Peng Su received his PhD (2008) degree from the College of Optical Sciences at the University of Arizona. He is currently a research associate professor there. His research focuses on developing advanced technologies for optical testing of large optical components and systems.

Todd Horne is an optomechanical engineer in the optics shop in the College of Optical Sciences at the University of Arizona.

Guido Brusa received his degree in physics in 1989 at the Universita' di Firenze (Italy). Since then he has held several appointments, including research astronomer from 1997 to 2002 at Osservatorio Astrofisico di Arcetri (Florence, Italy) and adaptive optics scientist at Steward Observatory and at the Large Binocular Telescope Observatory (Tucson, Arizona). His field of research is adaptive optics.

Jim H. Burge received his BS in engineering physics from Ohio State University in 1987, and his MS and PhD degrees in optical sciences in 1991 and 1993, from the University of Arizona. His current position is professor at the University of Arizona with joint appointments in optical sciences and astronomy. His interests are astronomical optics, optical fabrication and testing, optomechanics, and optical system engineering.